PNAS RESEARCH ARTICLE | PSYCHOLOGICAL AND COGNITIVE SCIENCES NEUROSCIENCE

Diffusion MRI–guided theta burst stimulation enhances memory and functional connectivity along the inferior longitudinal fasciculus in mild cognitive impairment

Yu-Chin Chen[a], Viet Ton That[a], Chidi Ugonna[a], Yilin Liu[a], Lynn Nadel[a,b,1], and Ying-hui Chou[a,b,c,1]

Contributed by Lynn Nadel; received July 27, 2021; accepted April 16, 2022; reviewed by Isabelle Buard, Joy Taylor, and Anthony Wagner

Mild cognitive impairment (MCI) during aging is often a harbinger of Alzheimer's disease, and, therefore, early intervention to preserve cognitive abilities before the MCI symptoms become medically refractory is particularly critical. Functional MRI–guided transcranial magnetic stimulation is a promising approach for modulating hippocampal functional connectivity and enhancing memory in healthy adults. Here, we extend these previous findings to individuals with MCI and leverage theta burst stimulation (TBS) and white matter tractography derived from diffusion-weighted MRI to target the hippocampus. Our preliminary findings suggested that TBS could be used to improve associative memory performance and increase resting-state functional connectivity of the hippocampus and other brain regions, including the occipital fusiform, frontal orbital cortex, putamen, posterior parahippocampal gyrus, and temporal pole, along the inferior longitudinal fasciculus in MCI. Although the sample size is small, these results shed light on how TBS propagates from the superficial cortex around the parietal lobe to the hippocampus.

transcranial magnetic stimulation | theta burst stimulation | mild cognitive impairment | magnetic resonance imaging | memory

Significance

Noninvasive theta burst stimulation (TBS) guided by brain white matter tractography is a promising approach to strengthen resting-state functional connectivity of the hippocampus and increase associative memory performance in individuals with mild cognitive impairment. With this approach, our findings add insight into how TBS propagates from the superficial stimulation site to the hippocampus along the inferior longitudinal fasciculus. Results of this study provide an innovative platform for developing a noninvasive hippocampal stimulation protocol that has great potential in enhancing memory function in mild cognitive impairment.

Mild cognitive impairment (MCI) lies somewhere between the expected cognitive decline of normal aging and Alzheimer's disease (AD). Although cognitive changes in individuals with MCI are not severe enough to interfere with daily function, people with MCI are at an increased risk of developing AD. Approximately 10 to 15% of individuals with MCI convert to AD every year (1). Individuals with amnestic MCI (aMCI), a subtype of MCI with memory impairment, have an even higher rate of conversion (1–3). Currently, pharmacological approaches are the mainstream of therapy for AD and MCI, and those interventions have demonstrated only moderate effects in reducing clinical symptoms for relatively short periods (4, 5). Therefore, we need nonpharmacological approaches, particularly treatment for memory dysfunction, for individuals with MCI before the cognitive impairments become medically refractory.

Cognitive impairments, especially in the domain of memory function, have been linked to significant abnormalities in various parts of the hippocampal network (6), which are among the earliest brain structures to develop neurodegenerative changes in AD (7). Previous brain imaging studies have shown that hippocampal volume loss (8), reduced hippocampal metabolism (9), and altered structural and resting-state functional connectivity (RSFC) of the hippocampal network (6, 10–12) are strongly associated with memory decline in AD. For example, patients with AD exhibit decreased RSFC between the hippocampus and several brain regions, such as frontal, parietal (e.g., precuneus), occipital, temporal, and limbic (e.g., cingulate and posterior cingulate gyrus) areas as well as insula and basal ganglia (e.g., putamen, globus pallidus, and caudate nucleus), compared to cognitively normal older adults (6, 10). Additionally, degradation in the hippocampal white matter tracks, as indexed by reduced fractional anisotropy in the fornix (11), and increased mean diffusivity of the anterior hippocampus (13) have also been reported in AD. Therefore, targeting the hippocampus might be a logical strategy to enhance memory function in individuals with MCI.

The impact of hippocampal stimulation on memory has been investigated with a broad variety of neurophysiological tools (14–16). Among those techniques, repetitive transcranial magnetic stimulation (rTMS) represents one of the most commonly used noninvasive brain stimulation tools because of its high acceptability in safety, tolerability, and efficacy to treat neurological and psychiatric disorders (17–19). However, rTMS can only directly excite cortical tissue of superficial brain regions. A major challenge in modulating deep brain regions such as the hippocampus is how to precisely deliver the magnetic pulses from the superficial stimulation site to the hippocampus.

Author affiliations: [a]Department of Psychology, University of Arizona, Tucson, AZ 85721; [b]Program in Cognitive Science, University of Arizona, Tucson, AZ 85721; and [c]Evelyn F McKnight Brain Institute, Tucson, AZ 85721

Author contributions: Y.-C.C., L.N., and Y.-h.C. designed research; Y.-C.C., V.T.T., and Y.-h.C. performed research; C.U. and Y.-h.C. contributed new reagents/analytic tools; Y.-C.C., C.U., Y.L., and Y.-h.C. analyzed data; Y.-C.C., C.U., L.N., and Y.-h.C. wrote the paper.

Reviewers: I.B., University of Colorado, Denver; J.T., Stanford University; and A.W., Stanford University

The authors declare no competing interest.

[1]To whom correspondence may be addressed. Email: nadel@arizona.edu or yinghuichou@email.arizona.edu.

This article contains supporting information online at http://www.pnas.org/lookup/suppl/doi:10.1073/pnas.2113778119/-/DCSupplemental.

Published May 20, 2022.

During the past few years, a number of rTMS studies have demonstrated that stimulating a superficial brain region (within the parietal lobe), which is functionally connected to the hippocampus, could modulate hippocampal activity and improve memory function in healthy adults (20, 21). In these studies, RSFC patterns were used to identify stimulation sites, but RSFC may not always be applicable for identifying a superficial stimulation site for older adults with MCI due to their altered functional connectivity. Here, we plan to leverage white matter tractography data from each individual with MCI and use the structural connectivity as a map to identify a superficial brain region that is anatomically connected with the hippocampus.

The goal of our study was to determine the effects of this tractography-guided hippocampal theta burst stimulation (TBS) on memory performance and RSFC in individuals with MCI. Additionally, we examined whether an excitatory or inhibitory hippocampal TBS protocol would be more beneficial for the enhancement of memory function in this population. Each participant underwent six TBS sessions: two excitatory intermittent TBS (iTBS), two inhibitory continuous TBS (cTBS), and two sham TBS on six different days (Fig. 1). The face–name (FNAME) associative memory data were collected in three TBS sessions (iTBS, cTBS, and sham TBS), and RSFC data were acquired in another three TBS sessions (iTBS, cTBS, and sham TBS) to prevent the influence of performing memory tasks on RSFC data. The order of the six sessions was randomized across participants. There were at least 5 d between TBS sessions to ensure an adequate washout period. Previous imaging studies have shown that theta-band oscillations generated by the hippocampus are responsible for phase coding, memory, and learning (22, 23). Therefore, mimicking theta-band oscillations with TBS has great potential in synchronizing and normalizing the hippocampal network and modulating memory function (24). Additionally, both iTBS and cTBS have been reported to enhance memory function and hippocampal activity (25, 26). In the current study, we hypothesized that iTBS, cTBS, or both active TBS conditions would improve associative memory performance and RSFC compared to sham TBS.

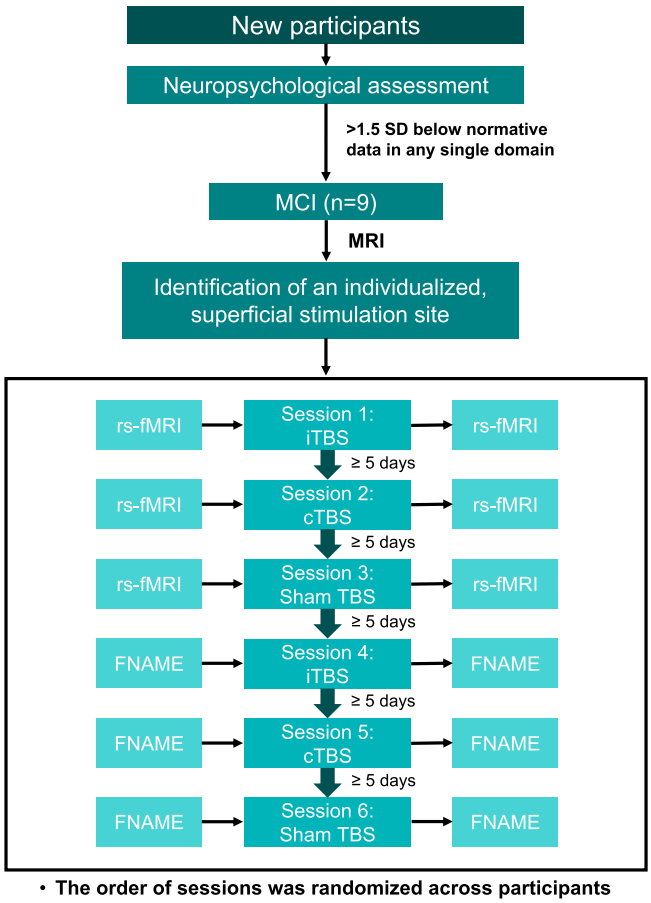

Fig. 1. Experimental design. A total of six TBS sessions were conducted on six different days with at least 5 d of a washout period between each TBS session. FNAME was administered in three TBS sessions (iTBS, cTBS, and sham TBS), and rs-fMRI was performed in another three TBS sessions (iTBS, cTBS, and sham TBS). The order of sessions was randomized across participants.

Results

Determination of Individual Stimulation Site with Diffusion-Weighted Imaging (DWI) Tractography Data. With the DWI tractography data from each participant, an individualized superficial stimulation site that was structurally connected to the cornu ammonis 1 (CA1), CA3, and dentate gyrus within the left hippocampus was identified (*Materials and Methods*). The superficial stimulation sites were located at the superior lateral occipital cortex ($n = 6$), superior parietal lobule ($n = 2$), and precuneus cortex ($n = 1$) in the left hemisphere (Table 1). These three superficial regions belong to the hippocampal–cortical network (27, 28), and each superficial stimulation site was structurally connected to the CA1, CA3, and dentate gyrus, which play an essential role in memory formation (29). An example of tractography maps with the CA1, CA3, and dentate gyrus as seeds from a single participant is illustrated in Fig. 2.

Enhancement of Associative Memory with TBS. Associative memory was assessed with the FNAME task (30) (Fig. 3*A*). Total memory score 1 (MTotal1), total memory score 2 (MTotal2), immediate retrieval, and delayed retrieval were measured by the number of items recalled after TBS minus the number of items recalled before TBS (Fig. 3*B*). Pairwise analyses of these memory scores revealed strong and significant correlations of MTotal1 and MTotal2 with other measures ($r = 0.83$ to 0.95, $P < 0.0001$; *SI Appendix*, Table S1). Changes in MTotal1 and MTotal2 of each participant following TBS conditions are reported in Table 2. The average MTotal1 score increased 5 ± 12.6 in iTBS, decreased 1.6 ± 7.6 in cTBS, and increased 0.7 ± 10.1 in sham TBS. The averaged MTotal2 score increased 4.2 ± 5 in iTBS, decreased 1.1 ± 4.8 in cTBS, and increased 0.9 ± 5.9 in sham TBS.

The normality assumption was checked by Shapiro–Wilk test for each data point, verifying an approximately normal distribution. The change scores of participant 6 were determined to be outliers by Grubb's test, Dixon's test, and Rosner's test. As can be seen in the Table 2, all the participants increased their associative memory scores after iTBS except for participant 6. Participant 6 decreased associative memory scores following iTBS but increased associative memory scores following cTBS. Interestingly, while the majority of the superficial stimulation sites from our research participants were located within the superior lateral occipital or superior parietal regions, the only exception was from participant 6; the superficial stimulation site determined for participant 6 was within the precuneus (Table 1). Previous functional MRI (fMRI) studies (31, 32) have found a negative correlation of activation patterns between the precuneus and the hippocampus. It is possible that exciting the precuneus with iTBS resulted in a decrease in hippocampal activation, and inhibiting the precuneus with cTBS increased

Table 1. Individualized superficial stimulation site identified by diffusion-weighted tractography linked to the left hippocampal subfields

SUB	MNI coordinates *x*, *y*, *z*			Location	Network	Coil orientation
1	−16	−68	56	Superior lateral occipital cortex	HCN, FPN	75
2	−32	−54	60	Superior parietal lobule	HCN, DMN	45
3	−12	−59	61	Superior lateral occipital cortex	HCN, FPN	30
4	−22	−78	38	Superior lateral occipital cortex	HCN, FPN	0
5	−20	−84	36	Superior lateral occipital cortex	HCN, FPN	105
6	−8	−74	48	Precuneus cortex	HCN, DMN	105
7	−16	−80	46	Superior lateral occipital cortex	HCN, FPN	120
8	−22	−60	68	Superior parietal lobule	HCN, DMN	45
9	−20	−59	60	Superior lateral occipital cortex	HCN, FPN	30

HCN, hippocampal–cortical network; DMN, default mode network; FPN, face perception network; MNI, Montreal Neurological Institute and Hospital coordinate system; SUB, subject.

hippocampal activation. Given that stimulating the precuneus might have resulted in an opposite effect on the hippocampus, data were analyzed with and without participant 6. Results of repeated measures ANOVA for associative memory performance and RSFC with the outlier were included in *SI Appendix*, Tables S2 and S3 and Fig. S1.

A repeated measures ANOVA revealed that the TBS effects on MTotal1, MTotal2, immediate retrieval, and delayed retrieval scores were all significant (Table 3). Post hoc analyses showed that iTBS had stronger effects than cTBS on both MTotal2 (i.e., immediate retrieval and delayed retrieval; $P < 0.05$) and delayed retrieval ($P < 0.05$), with multiple testing correction via false discovery rate (FDR) (33). Although the contrasts of iTBS versus sham TBS did not survive the correction for multiple comparisons, these effect sizes (Cohen's *d*) were greater than 0.99, which exceeded Cohen's convention for large effects.

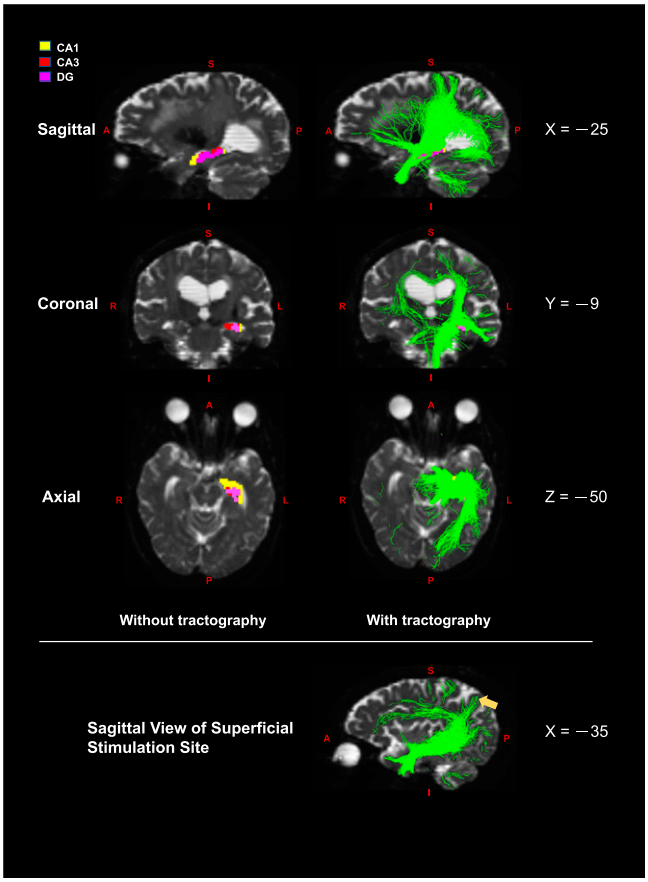

Fig. 2. The sagittal ($x = -25$), coronal ($y = -9$), and axial ($z = -50$) views of diffusion-weighted MRI tractography with the three hippocampal subfields, CA1 (yellow), CA3 (red), and dentate gyrus (DG, pink) as a seed. The figures at each row are the same slices with and without tractography. The right figures illustrate the overlays of three tractography maps of CA1, CA3, and DG. The yellow arrow in the bottom figure ($x = -35$) points to the determined superficial site; A = anterior; L = left; I = inferior; P = posterior; R = right; S = superior.

Increased Functional Connectivity along the Hippocampal Pathway. We examined the TBS effects on changes in functional connectivity (ΔF) from each participant's superficial stimulation site to other brain regions with a one-way repeated measures ANOVA and post hoc analyses corrected for multiple comparisons with the FDR.

Repeated measures ANOVA and post hoc analyses revealed a significant TBS effect on RSFC between the superficial stimulation site and seven brain areas, including the bilateral occipital fusiform gyrus, the bilateral frontal orbital cortex, the right posterior parahippocampal gyrus, the right temporal pole, and the right putamen (Table 4). Most of these brain regions are connected to the superficial stimulation site and the hippocampus through the inferior longitudinal fasciculus (ILF) and corpus callosum (*Discussion*). In general, iTBS increased functional connectivity, while the changes in functional connectivity following cTBS were inconsistent across brain regions (Table 4).

Using the whole left or right hippocampus as a region of interest (ROI) did not reveal a significant TBS effect ($P = 0.698$ for the left hippocampus and $P = 0.623$ for the right hippocampus), indicating heterogeneous roles of subfields within the hippocampus. We conducted exploratory analyses with multiple testing correction via FDR using subfields of the left and right hippocampi as ROIs and found that, compared to sham TBS, 1) iTBS increased functional connectivity between the superficial stimulation site and the left CA1 ($P = 0.016$) and left hippocampal fissure ($P = 0.05$), and 2) cTBS increased functional connectivity between the superficial stimulation site and the right hippocampal fissure ($P = 0.033$). These findings suggested that TBS could be used to modulate changes in RSFC between the superficial stimulation site and the hippocampal subfields in both hemispheres.

Discussion

The present study aimed to determine whether a single session of tractography-guided TBS could be used to modulate the hippocampal network and enhance associative memory function in individuals with MCI. First, we were able to identify superficial stimulation sites with the DWI white matter tractography data for each participant. Second, iTBS significantly

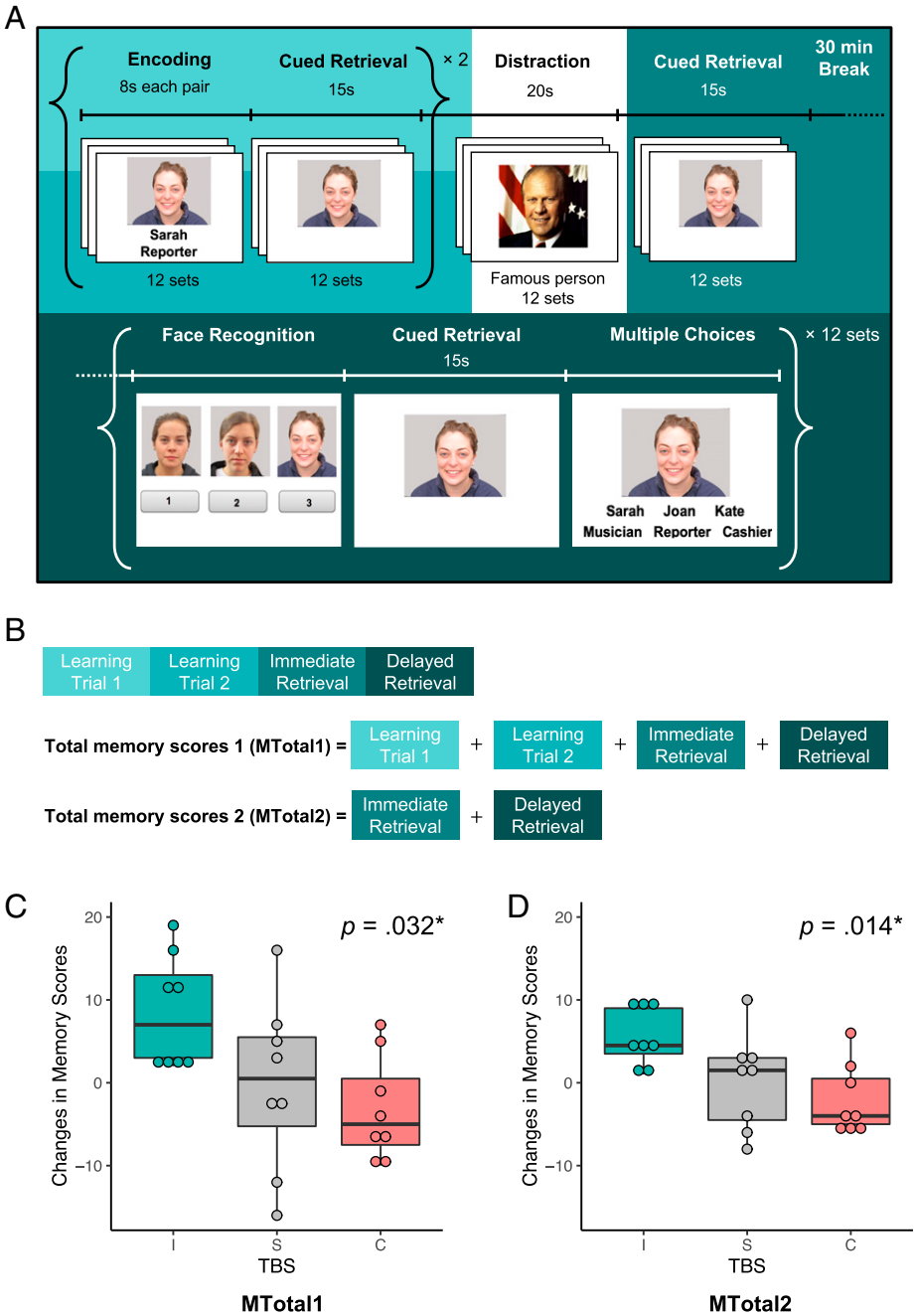

Fig. 3. The FNAME task and the associative memory results. (*A*) During the encoding phase, participants were required to memorize 12 sets of faces, names, and occupations. After each encoding session, they had to retrieve names and occupations by face cues immediately (i.e., learning trial 1 and learning trial 2). Followed by two encoding sessions, 12 faces of famous people were presented (i.e., distractions). After the distractions, participants were assessed with cued retrieval (i.e., immediate retrieval). After a 30-min break, participants underwent additional retrieval tasks (i.e., delayed retrieval). (*B*) The MTotal1 was composed of learning trial 1, learning trial 2, immediate retrieval, and delayed retrieval. The MTotal2 included immediate retrieval and delayed retrieval. (*C* and *D*) The box plots revealed significant TBS effects on associative memory MTotal1 (*C*) scores (F[2, 14] = 4.47, P = 0.032) and MTotal2 (*D*) scores (F[2, 14] = 5.93, P = 0.014); I, intermittent TBS; C, continuous TBS; S, sham TBS.

increased associative memory scores compared to cTBS. Third, relative to sham TBS, iTBS significantly increased the RSFC between the superficial stimulation site and multiple brain regions, including the occipital fusiform bilaterally, the frontal orbital cortex bilaterally, the right putamen, the right posterior parahippocampal gyrus, the right temporal pole, and several hippocampal subfields.

The majority of the brain regions that exhibited increased RSFC with the superficial stimulation site are structurally connected to the hippocampus via the ILF. According to a previous diffusion tensor imaging study (34), more than 40% of hippocampal connections to other brain regions pass through the ILF. The ILF connects the temporal and occipital lobes and supports functions associated with the ventral visual stream, such as face recognition, visual memory, object recognition, and semantic processes (35). The fusiform gyrus connects to the anterior temporal regions through one of the ILF branches (35) and plays an important role in face perception (36, 37). In addition to face perception, the fusiform gyrus is also involved in the processing of words and names (38). The temporal pole is located at the anterior part of the ILF and is further connected to the frontal orbital cortex by the uncinate fasciculus

Table 2. Changes of associative memory scores following excitatory iTBS, inhibitory cTBS, and sham TBS conditions

		MTotal1			MTotal2		
SUB	MCI/ aMCI	iTBS	cTBS	Sham	iTBS	cTBS	Sham
1	aMCI	11	−9	−3	5	−6	−6
2	aMCI	12	−4	16	10	−4	10
3	aMCI	3	−1	−2	4	0	2
4	aMCI	2	7	7	4	6	1
5	MCI	16	−6	−16	9	−5	−8
6	MCI	−24	11	8	−6	6	7
7	aMCI	19	−10	5	9	−5	3
8	aMCI	3	−7	−12	2	−4	−4
9	aMCI	3	5	3	1	2	3

SUB, subject.

(35, 39). These anterior portions of the ILF are commonly disrupted in neurodegenerative diseases (40). The temporal pole involves retrieving and storing proper names (41), allowing the individual to be identified and remembered. It completes the process of face recognition by linking representations with semantic information specific to each individual (42). The frontal orbital cortex is also a face-selective region (43). It is capable of discriminating face from nonface stimuli (44), classifying social and emotional reinforcement signals from faces, and modulating the memory processes of FNAME associations, which are mediated by the hippocampus (43, 45). The putamen is located at the edges of the ILF and the inferior fronto-occipital fasciculus (46) and is connected to the hippocampus (34). Activation of the putamen reflects involvement in visual and orthographic processing as well as language processing (47). Finally, another anterior termination of the ILF involves the parahippocampal gyrus (48). Although it is believed that the parahippocampal gyrus is more important in visuospatial recognition (e.g., scenes and places) and contextual mnemonic processes (49), activation of the parahippocampal cortex has also been found during successful encoding and retrieval of associative information (50).

In the exploratory analyses using the hippocampal subfields in both hemispheres as ROIs, our data showed that, compared to sham TBS, iTBS increased RSFC between the superficial stimulation site and the left CA1 and hippocampal fissure, and cTBS increased RSFC between the superficial stimulation site and the right hippocampal fissure. The CA1 plays several essential roles in memory formation (51, 52), including serving as a mismatch detector, comparing current experience with expectations generated by previously stored data (53, 54). Atrophy/lesions of the CA1 contribute to memory deficits in AD (55) and other amnestic disorders (56, 57). The hippocampal fissure (also known as hippocampal sulcus) separates the CA2, CA3, and dentate gyrus from the CA1 and subiculum (58), and impairments in its function have been implicated in AD, medial temporal lobe atrophy, and other memory disorders (59, 60). Overall, findings of our study together with previous evidence suggest that the ILF may be the pathway through which effective TBS is transmitted down to the hippocampus. Furthermore, the effect of TBS on FNAME associative memory may be accounted for by modulated RSFC along the ILF, although future studies will be needed to elucidate how these brain regions coordinate and contribute specifically to the associative memory capacities engaged by the FNAME task.

The application of TBS is relevant to populations with memory impairment because theta-band oscillations generated by the hippocampus appear to be responsible for phase coding, memory, and learning (23, 24). As such, using TBS to mimic theta-band oscillations has great potential in synchronizing and normalizing the hippocampal network. In our study, the majority of participants showed improved memory performance and increased RSFC following excitatory iTBS. Although three participants also increased their memory scores after receiving inhibitory cTBS, this effect was not significant. Previous TBS studies stimulating the primary motor cortex have found that iTBS usually enhances cortical excitability, while cTBS suppresses cortical excitability, presumably reflecting long-term potentiation and long-term depression effects, respectively (61, 62). TBS studies targeting the left parietal lobe observed increased functional connectivity in cognitive networks following iTBS and decreased functional connectivity in response to cTBS (63). Our study is in agreement with these previous findings and suggests that iTBS might cause memory enhancement compared to cTBS.

While findings of our study with a small sample size are encouraging, limitations of the study should also be noted. The variability in response to the different stimulation regimens is perplexing (64). Factors such as medication status, exercise/fitness, genotype, stimulation intensity, and number of TBS sessions warrant systematic examinations in future studies. Additionally, the effects of iTBS on RSFC did not appear selective to the hippocampus only and were observed in seven other brain regions connected to the superficial stimulation site through the ILF. Although our exploratory analyses using the hippocampal subfields in both hemispheres as ROIs showed

Table 3. Changes in memory scores following TBS (n = 8): Results of repeated measures ANOVA with multiple comparisons corrected by FDR

Changes in memory scores (post–pre)	ANOVA (F, P)	iTBS ($M \pm S$)	cTBS ($M \pm S$)	Sham TBS ($M \pm S$)	I versus S (P and *effsize*)	C versus S (P and *effsize*)	I versus C (P and *effsize*)
MTotal1	4.5, 0.03*	8.6 ± 6.7	−3.1 ± 6.3	−0.3 ± 10.4	0.12, 1.02	0.45, −0.34	0.09, 1.80
MTotal2	5.9, 0.01*	5.5 ± 3.4	−2.0 ± 4.2	0.1 ± 5.8	0.07, 1.12	0.36, −0.42	0.048*, 1.95
Immediate retrieval	3.9, 0.04*	2.8 ± 2.1	−1.0 ± 2.1	−0.1 ± 3.1	0.10, 1.10	0.51, −0.30	0.10, 1.54
Delayed retrieval	5.9, 0.01*	2.7 ± 2.0	−1.0 ± 2.0	0.3 ± 3.0	0.07, 0.99	0.31, −0.49	0.046*, 1.88

Effsize, effect size; C, cTBS; I, iTBS; S, sham TBS; M, mean; S, standard deviation.
*$P < 0.05$

Table 4. Changes in functional connectivity between each participant's superficial stimulation site and other brain regions following TBS ($n = 8$): Results of repeated measures ANOVA with multiple comparisons corrected by FDR

Connected regions	ANOVA (F, P)	iTBS ($M \pm S$)	cTBS ($M \pm S$)	Sham TBS ($M \pm S$)	I versus S (P and *effsize*)	C versus S (P and *effsize*)	I versus C (P and *effsize*)
L frontal orbital cortex	11.7, 0.001*	−0.02 ± 0.17	0.14 ± 0.31	−0.22 ± 0.17	0.004*, 1.18	0.004*, 1.43	0.16, −0.62
R posterior parahippocampal gyrus	7.9, 0.005*	0.14 ± 0.15	0.01 ± 0.20	−0.19 ± 0.21	0.009*, 1.86	0.12, 1.01	0.12, 0.77
R putamen	7.0, 0.008*	0.13 ± 0.12	−0.04 ± 0.18	−0.12 ± 0.15	0.02†, 1.83	0.27, 0.48	0.08, 1.13
L occipital fusiform gyrus	6.9, 0.008*	0.02 ± 0.23	−0.05 ± 0.11	−0.31 ± 0.24	0.037†, 1.40	0.037†, 1.36	0.41, 0.42
R temporal pole	4.8, 0.026†	0.07 ± 0.33	−0.07 ± 0.20	−0.27 ± 0.38	0.025†, 0.97	0.16, 0.67	0.31, 0.52
R occipital fusiform gyrus	4.4, 0.034†	0.08 ± 0.20	−0.04 ± 0.24	−0.26 ± 0.34	0.035†, 1.20	0.24, 0.76	0.30, 0.51
R frontal orbital cortex	4.3, 0.034†	0.01 ± 0.20	0.03 ± 0.30	−0.23 ± 0.18	0.032†, 1.26	0.06, 1.07	0.82, −0.11
L hippocampal fissure	4.7, 0.028†	0.02 ± 0.09	−0.11 ± 0.12	−0.26 ± 0.24	0.05†, 1.52	0.21, 0.79	0.05†, 1.18
L CA1	3.4, 0.06	0.19 ± 0.23	−0.01 ± 0.21	−0.07 ± 0.23	0.016†, 1.17	0.60, 0.29	0.23, 0.92
R hippocampal fissure	4.5, 0.031†	0.07 ± 0.26	0.14 ± 0.26	−0.11 ± 0.11	0.14, 0.91	0.03†, 1.27	0.46, 0.28

The brain regions were defined by the Harvard–Oxford cortical and subcortical structural atlases. The hippocampal subfields were defined by FreeSurfer v6.0 segmentations. Effsize, effect size; C, cTBS; I, iTBS; S, sham TBS; L, left; R, right.
*$P < 0.01$.
†$P < 0.05$.

that, compared to the sham TBS, active TBS conditions increased RSFC between the superficial stimulation site and the hippocampal subfields, we cannot rule out the possibility that the observed seven other brain regions might also contribute to the alteration of associative memory performance following iTBS. Potential contributions of these brain regions to memory enhancement following iTBS should be explored further in future research.

In conclusion, the results of our study support our hypothesis that iTBS is the active TBS condition that has a significant effect on associative memory and RSFC compared to cTBS and sham TBS conditions. TBS guided by DWI tractography has great potential for modulating the hippocampal network via the ILF and enhancing associative memory in individuals with MCI. Our experiment shows that excitatory iTBS is more beneficial for associative memory enhancement than inhibitory cTBS. Our findings can be used to guide future research design in MCI or AD to leverage the MRI data for planning stimulation sites and monitoring TBS therapeutic effects.

Materials and Methods

Experimental Designs. The aims of the study were to examine TBS effects on memory and RSFC of the hippocampal network in individuals with MCI. As mentioned earlier, there were three conditions: inhibitory cTBS, excitatory iTBS, and sham TBS. The outcome measures, including associative memory performance and RSFC, were acquired immediately before and immediately after each TBS session. The interval between the TBS session and the MRI scanning was 5.0 ± 2.2 min because the MRI scanner was adjacent to the TMS room. The FNAME associative memory task was administered in three TBS sessions (iTBS, cTBS, and sham TBS), and resting-state fMRI (rs-fMRI) was performed in another three TBS sessions (iTBS, cTBS, and sham TBS), yielding a total of six TBS sessions on six different days (Fig. 1). The order of the six sessions was randomized across participants. There were at least 5 d between TBS sessions to ensure an adequate washout period. Participants were blinded to the order of TBS sessions.

Participants. Nine right-handed older adults aged between 65 and 74 y old (70 ± 3 y, five females) participated in our study. Despite self-reported cognitive issues among the participants, whose average education was 16.7 ± 2.1 y, they were still able to independently perform daily living activities, such as preparing food, dressing, and bathing, without assistance. All participants were free from any other known neurological and psychiatric conditions (e.g., previous seizure history, Parkinson's disease, stroke, dementia, or depression). Participants were classified as individuals with MCI based on testing scores derived from the Uniform Data Set version 3 (UDS3) neuropsychological battery. None of them was taking antipsychotic medications nor had they recently experienced withdrawal from drugs. Participants were screened for TMS safety with the latest guidelines (65–68). There were no contraindications to MRI or TMS among the participants. Participants in the study were native speakers of English. Both auditory and visual acuity were normal or corrected to normal. This study was approved by the Institutional Review Board of University of Arizona. Each participant voluntarily consented to participate and was paid for their participation.

Neuropsychological Examinations. The UDS3 neuropsychological battery, developed by the National Alzheimer's Coordinating Center, and the Rey Auditory Verbal Learning Test were administered to measure cognitive function (69, 70). The UDS3 neuropsychological battery is composed of multiple cognitive domains, including memory, executive functioning, attention, processing speed, and language. The performance scores were calculated by a regression-based norms calculator, providing estimated z scores, which were adjusted for age, sex, and education. Participants were classified as having "MCI" if their z scores were 1.5 SD below the mean of the normative data in any cognitive domain (71, 72). Participants were further categorized as "aMCI" if they had impairment in the memory domain.

TMS Protocols. TMS was delivered using the MagVenture MagPro ×100 stimulator (MagVenture Inc.) equipped with figure-of-eight magnetic coils (MagVenture C-B60 and Cool-B65 coils) and an active cooling system. In this study, we used TBS protocols, which mimic the natural endogenous "theta rhythms" of the human brain for the modulation of cortical plasticity (24, 62, 73). TBS, a more efficient and enduring protocol than conventional repetitive TMS, consists of high-frequency bursts (three pulses at 50 Hz) repeated five times per second

(i.e., 30 stimuli within 2 s). There are two types of TBS protocols (i.e., cTBS and iTBS), and both protocols consisted of 600 stimuli. For the iTBS protocol, the 30 stimuli were applied every 2 s with an 8-s interval between each train (i.e., 20 trains in total taking ∼192 s). For the cTBS protocol, the 30 stimuli were applied continuously without intertrain intervals (i.e., 20 trains in total taking 40 s). The iTBS protocol is usually associated with facilitation in neural activity, while the cTBS protocol typically leads to a suppression of synaptic transmission (24, 62). A single session of TBS induces transient effects in the targeted brain structures/networks that tend to last ∼30 to 60 min.

Each participant could have a different level of sensitivity to the magnetic fields generated by the TMS. Therefore, we used single-pulse TMS to determine the lowest stimulation intensity required for each participant. Stimulation intensity was adjusted based on each individual's resting motor threshold (RMT). The RMT was estimated with the TMS Motor Threshold Assessment Tool 2.0 (http://www.clinicalresearcher.org/software.htm) that uses maximum-likelihood parameter estimation by sequential testing strategy without the need for a priori information (74). The estimated RMT was further verified by eliciting at least three motor-evoked potentials of 50-μV peak-to-peak amplitude of the right abductor pollicis brevis muscle measured with an electromyography machine in six consecutive stimulations on the hotspot of the left primary motor cortex. Once the RMT was determined, the stimulation intensity for TBS was set to 70% of individual RMT (75). Subsequently, we located this preplanned superficial stimulation target by coregistering the participant's head, structural T1-weighted MRI image, and TMS coil in the same space using a TMS stereotactic three-dimensional (3D) navigation system (LOCALITE). When coregistration was complete, the TMS stereotactic system provided real-time feedback of the coil location and recorded the coil position and orientation relative to the head. In our sham TBS condition, we used a sham TMS coil designed for blinding purposes. The sham coil has a magnetic blockage to block the stimulation but still generates stimulation sounds and vibrating sensations (76). We followed up-to-date safety guidelines (65–68) to minimize side effects. Participants wore earplugs to protect their hearing.

Determination of an Individualized Superficial Stimulation Site. Both diffusion-weighted and T1 structural MRI data were used to determine the individualized superficial stimulation site with the following steps. First, the diffusion data were preprocessed to reduce artifacts and noise. We removed the Gibbs ringing artifacts (77) and used FMRIB Software Library (FSL) TOPUP to estimate and correct susceptibility-induced distortions using reverse encoded DWI data (78). We then applied FSL's eddy to correct for eddy current–induced distortions and head movement (79). The corrected data were denoised using local principal component analysis (80). The final preprocessing step applied bias field correction to the dataset using the ANTs package (81). Second, we used FreeSurfer (https://surfer.nmr.mgh.harvard.edu) for anatomical preprocessing and segmentation of hippocampal subfields. The left hippocampus was segmented into 13 subfields using FreeSurfer 6.0 (82). Among the 13 subfields, the CA1, CA3, and dentate gyrus within the left hippocampus were selected as the ROIs because these hippocampal subfields are involved in memory formation (29, 83). Third, tractography analysis was performed on the preprocessed diffusion data using MRtrix (https://github.com/MRtrix3) to generate a total of three white matter tractography maps from each of the ROIs for each participant. Multishell, multitissue constrained spherical deconvolution (MSMT-CSD), one of the high angular resolution diffusion imaging (HARDI) modeling techniques, was used to resolve the crossing fibers limitation of standard diffusion tensor imaging. MSMT-CSD leverages multishell (multiple b value) DWI data to estimate a multitissue orientation distribution function, which takes into account the unique b value dependency of different tissue types, white matter, gray matter, and cerebrospinal fluid (CSF), in the brain. This procedure produces more reliable white matter/gray matter/CSF volume fraction maps and significantly raises the precision of fiber orientations (84), leading to more reliable tractography results. MSMT-CSD can be implemented in MRtrix3 by using the dwi2fod dhollander and dwi2fod msmt_csd commands. Streamlines were generated using the MRtrix3's tckgen command. The tckgen function generated a new streamline at each iteration by repeatedly sampling from the voxel-wise principal diffusion direction computed in dwi2fod. The total value of 1,000,000 iterations was executed. Fourth, three tractography maps were generated and used to determine a superficial stimulation site for each participant (Fig. 2). The following criteria were used to determine the optimal superficial stimulation site for each participant: 1) the superficial site was within 3 cm from the scalp, 2) the superficial site was structurally connected to the CA1, CA3, and dentate gyrus, and 3) the superficial site was within the parietal and occipital regions. We were able to identify one superficial stimulation site for each participant with these criteria. Once the stimulation target was determined, we then used SimNIBS 2.1 (http://simnibs.de/start) to estimate the optimal stimulation orientation (85, 86). Finally, the image data and the target coordinate were imported to the real-time TMS stereotactic navigation system (Localite GmbH).

We also performed seed-based functional connectivity analysis with the FSL/FEAT software for determining the RSFC-guided superficial stimulation site. The threshold was $Z > 3.1$ with a corrected cluster threshold of $P < 0.001$ (87). We could identify the superficial stimulation sites in seven out of the nine participants. The hippocampal RSFC to the parietal or occipital regions for participants 4 and 6 was -0.245 ± 0.205 ($Z = 2.1$) and -0.209 ± 0.085 ($Z = 1.2$), respectively, which did not survive the correction of multiple comparisons. For these two participants (4 and 6), although the hippocampus and the superficial stimulation sites were structurally connected (as estimated by the tractography data), the RSFC between these two regions was very low. Notably, six (1, 3, 5, 7, 8, and 9) of the remaining seven participants showed consistent results between RSFC-based and tractography-based strategies. For participant 2, the tractography-based stimulation site was within the superior parietal lobe, and the RSFC-guided site was within the superior lateral occipital cortex.

MRI Data Acquisition. MRI images were acquired by a MAGNETOM Skyra 3 Tesla MRI scanner (Siemens Medical Systems) with a 32-channel receiver head coil. Foam pads were applied to prevent head motion. The structural MRI protocol included T1-MPRAGE (a 3D gradient echo pulse sequence, T1-weighted) with a repetition time (TR) of 2,530.0 ms, echo time (TE) of 3.3 ms, inversion time (TI) of 1,100 ms, flip angle (FA) of 7°, field of view (FoV) of 256 mm, and parallel imaging (GRAPPA 2) resolution of 1.0 × 1.0 × 1.0 mm and a T2-FLAIR (a fluid-attenuated inversion recovery MRI sequence, T2-weighted) with a TR of 6,700.0 ms, TE of 101 ms, TI of 2,500 ms, FA of 120°, FoV of 256 mm, and parallel imaging (GRAPPA 2) resolution of 1.0 × 1.0 × 2.5 mm. Diffusion-weight MRI (single-shot parallel and multiband dual-spin-echo echo-planar imaging [EPI] pulse sequence) parameters included an FoV of 256 mm; in-plane matrix size of 128 × 128; in-plane acceleration factor of 2; multiband factor of 2; TE of 119 ms; TR of 3,700 ms; slice thickness of 2 mm; voxel size of 2 mm^3; $b = 0$, 1,000, 2,000, and 3,000 s/mm^2 as three shell acquisitions for further HARDI approach; number of diffusion-encoding directions of 60; and a scan time of 9 min. To reduce susceptibility-induced distortions, two $b = 0$ images with identical parameters to the main DWI sequence were acquired but with opposing phase-encoding polarity. Finally, an rs-fMRI (T2*-weighted gradient-echo EPI pulse sequence, FoV = 240 mm, TR = 3,000 ms, TE = 36 ms, FA = 90°, in-plane acquisition matrix size = 160 × 160, voxel size = 1.5 mm^3, and multiband factor = 2; scan time of 8 min) was acquired to evaluate changes in functional connectivity in response to TBS. During the scans, participants were asked to stay awake and hold still, keep their eyes focused on a cross hair, and let their thoughts come and go as they will.

Outcome Measures and Statistical Analyses. Both associative memory and RSFC were used to determine the individual response to each TBS condition. We used RSFC to evaluate the deliverability of TMS to the hippocampus (12, 88).

FNAME memory test. The FNAME was designed as an assessment tool for associative memory function because it is sensitive to subtle memory changes, and its score is correlated with early amyloid-β deposition (30, 89). The FNAME is composed of 12 face-name-occupation pairs, with two learning trials, two immediate recall trials, a short-delayed recall after distraction (identifying 12 famous celebrities), and a 30-min delayed recall (Fig. 3*A*). Participants were instructed to associate a series of unfamiliar faces, common first names, and common occupations and to recall the name and occupation of each face in the recall trials. In the long-delayed recall, elements included familiarity assessed by recognizing the previously presented faces among two other new faces, face cued retrieval, and 30-min delayed recall (Fig. 3*A*). We adopted two existing FNAME versions from a previous study (30) and created four new versions, matching the proportion of genders, ages, races, smile/neutral expressions, and syllable counts of names and occupations with the previous two versions. Adult faces and names were obtained from the Face Database (90) and popular baby names from the

Social Security website. We performed the intraclass correlation coefficient (ICC) analysis to examine the parallel-forms reliability across the six versions of the FNAME test. Eleven younger adults (age = 24.6 ± 5.5 y, 36% female) took all the six versions of the FNAME test in a randomized order. Analysis of the data using a single-measurement, absolute agreement, two-way mixed-effects model revealed an ICC of 0.75 (95% confidence interval of 0.55, 0.91), indicating moderate to good parallel-forms reliability across the six FNAME test versions.

The MTotal1 of FNAME was composed of learning trial 1, learning trial 2, immediate retrieval, and delayed retrieval (Fig. 3*B*). The MTotal2 included immediate retrieval and delayed retrieval. The dependent variables (i.e., MTotal1, MTotal2, immediate retrieval, and delayed retrieval) reflect the changes in number of items recalled following TBS minus the number of items recalled before TBS. All the data were checked for normality with the Shapiro–Wilk normality test. We used a one-way repeated measures ANOVA to examine TBS effects on associative memory performance. Post hoc analyses with pairwise comparisons between conditions were corrected by the FDR.

fMRI and statistical analyses. The rs-fMRI data were acquired immediately before and after each TBS session for functional connectivity analysis, which was performed by CONN toolbox (https://www.nitrc.org/projects/conn) (91). One hundred and six brain regions defined by the Harvard–Oxford cortical and subcortical structural atlases, 26 (13 × 2 hemispheres) FreeSurfer-segmented hippocampal subfields, and the superficial stimulation sites were included for the seed-based ROI-to-ROI functional connectivity analyses. The voxel sizes of our rs-fMRI data are 1.5 mm^3. Unsmoothed preprocessed data were used in the analyses. A Fisher-transformed correlation coefficient (*Z*) was calculated to evaluate the changes of functional connectivity associated with the ROIs. Repeated measures ANOVAs were used to analyze changes following TBS in RSFC with multiple comparisons corrected by the FDR. Statistical analyses were performed using RStudio (RStudio, Inc.), Python 3, and MATLAB (MathWorks).

Data Availability. Anonymized MRI data that support the findings of this study are available from the corresponding author, Y.-h.C., upon reasonable request. All other data are included in the manuscript and/or *SI Appendix*.

ACKNOWLEDGMENTS. We thank Dr. Ying-Zu Huang for advising on the TBS protocols and the research design, Dr. Adam Bernstein for providing the singularity image that helped with the diffusion-weighted MRI preprocessing, and John Fritsche and Jonny Baham for preparing the FNAME versions. This work was supported by the National Institutes of Health R01 AG062543 (Y.-h.C.) and R21 AG077153 (Y.-h.C.).

1. P. Fischer *et al.*, Conversion from subtypes of mild cognitive impairment to Alzheimer dementia. *Neurology* **68**, 288–291 (2007).
2. T. L. Michaud, D. Su, M. Siahpush, D. L. Murman, The risk of incident mild cognitive impairment and progression to dementia considering mild cognitive impairment subtypes. *Dement. Geriatr. Cogn. Disord. Extra* **7**, 15–29 (2017).
3. K. Schmidtke, S. Hermeneit, High rate of conversion to Alzheimer's disease in a cohort of amnestic MCI patients. *Int. Psychogeriatr.* **20**, 96–108 (2008).
4. A. A. D. T. Abeysinghe, R. D. U. S. Deshapriya, C. Udawatte, Alzheimer's disease; a review of the pathophysiological basis and therapeutic interventions. *Life Sci.* **256**, 117996 (2020).
5. D. S. Knopman *et al.*, Alzheimer disease. *Nat. Rev. Dis. Primers* **7**, 33 (2021).
6. J. Xue *et al.*, Altered directed functional connectivity of the hippocampus in mild cognitive impairment and Alzheimer's disease: A resting-state fMRI study. *Front. Aging Neurosci.* **11**, 326 (2019).
7. P. V. Arriagada, J. H. Growdon, E. T. Hedley-Whyte, B. T. Hyman, Neurofibrillary tangles but not senile plaques parallel duration and severity of Alzheimer's disease. *Neurology* **42**, 631–639 (1992).
8. F. Shi, B. Liu, Y. Zhou, C. Yu, T. Jiang, Hippocampal volume and asymmetry in mild cognitive impairment and Alzheimer's disease: Meta-analyses of MRI studies. *Hippocampus* **19**, 1055–1064 (2009).
9. E. J. Choi *et al.*, Glucose hypometabolism in hippocampal subdivisions in Alzheimer's disease: A pilot study using high-resolution ^{18}F-FDG PET and 7.0-T MRI. *J. Clin. Neurol.* **14**, 158–164 (2018).
10. M. Filippi, F. Agosta, Structural and functional network connectivity breakdown in Alzheimer's disease studied with magnetic resonance imaging techniques. *J. Alzheimers Dis.* **24**, 455–474 (2011).
11. K. Kantarci, Fractional anisotropy of the fornix and hippocampal atrophy in Alzheimer's disease. *Front. Aging Neurosci.* **6**, 316 (2014).
12. Y. I. Sheline, M. E. Raichle, Resting state functional connectivity in preclinical Alzheimer's disease. *Biol. Psychiatry* **74**, 340–347 (2013).
13. B. Zhang, Y. Xu, B. Zhu, K. Kantarci, The role of diffusion tensor imaging in detecting microstructural changes in prodromal Alzheimer's disease. *CNS Neurosci. Ther.* **20**, 3–9 (2014).
14. N. Suthana *et al.*, Memory enhancement and deep-brain stimulation of the entorhinal area. *N. Engl. J. Med.* **366**, 502–510 (2012).
15. X. Liu *et al.*, Optogenetic stimulation of a hippocampal engram activates fear memory recall. *Nature* **484**, 381–385 (2012).
16. J. X. Wang, J. L. Voss, Long-lasting enhancements of memory and hippocampal-cortical functional connectivity following multiple-day targeted noninvasive stimulation. *Hippocampus* **25**, 877–883 (2015).
17. Y. H. Chou, P. T. Hickey, M. Sundman, A. W. Song, N. K. Chen, Effects of repetitive transcranial magnetic stimulation on motor symptoms in Parkinson disease: A systematic review and meta-analysis. *JAMA Neurol.* **72**, 432–440 (2015).
18. Y. H. Chou, V. Ton That, M. Sundman, A systematic review and meta-analysis of rTMS effects on cognitive enhancement in mild cognitive impairment and Alzheimer's disease. *Neurobiol. Aging* **86**, 1–10 (2020).
19. L. De Risio *et al.*, Recovering from depression with repetitive transcranial magnetic stimulation (rTMS): A systematic review and meta-analysis of preclinical studies. *Transl. Psychiatry* **10**, 393 (2020).
20. J. X. Wang *et al.*, Targeted enhancement of cortical-hippocampal brain networks and associative memory. *Science* **345**, 1054–1057 (2014).
21. A. S. Nilakantan *et al.*, Network-targeted stimulation engages neurobehavioral hallmarks of age-related memory decline. *Neurology* **92**, e2349–e2354 (2019).
22. A. Goyal *et al.*, Functionally distinct high and low theta oscillations in the human hippocampus. *Nat. Commun.* **11**, 2469 (2020).
23. H. Zhang, J. Jacobs, Traveling theta waves in the human hippocampus. *J. Neurosci.* **35**, 12477–12487 (2015).
24. A. Suppa *et al.*, Ten years of theta burst stimulation in humans: Established knowledge, unknowns and prospects. *Brain Stimul.* **9**, 323–335 (2016).
25. M. S. Hermiller, S. VanHaerents, T. Raij, J. L. Voss, Frequency-specific noninvasive modulation of memory retrieval and its relationship with hippocampal network connectivity. *Hippocampus* **29**, 595–609 (2019).
26. M. S. Hermiller, Y. F. Chen, T. B. Parrish, J. L. Voss, Evidence for immediate enhancement of hippocampal memory encoding by network-targeted theta-burst stimulation during concurrent fMRI. *J. Neurosci.* **40**, 7155–7168 (2020).
27. L. E. Frank, C. R. Bowman, D. Zeithamova, Differential functional connectivity along the long axis of the hippocampus aligns with differential role in memory specificity and generalization. *J. Cogn. Neurosci.* **31**, 1958–1975 (2019).
28. J. L. Vincent *et al.*, Coherent spontaneous activity identifies a hippocampal-parietal memory network. *J. Neurophysiol.* **96**, 3517–3531 (2006).
29. T. Hainmueller, M. Bartos, Dentate gyrus circuits for encoding, retrieval and discrimination of episodic memories. *Nat. Rev. Neurosci.* **21**, 153–168 (2020).
30. D. M. Rentz *et al.*, Promising developments in neuropsychological approaches for the detection of preclinical Alzheimer's disease: A selective review. *Alzheimers Res. Ther.* **5**, 58 (2013).
31. M. Tahmasian *et al.*, The lower hippocampus global connectivity, the higher its local metabolism in Alzheimer disease. *Neurology* **84**, 1956–1963 (2015).
32. S. Zhang, C. S. Li, Functional connectivity mapping of the human precuneus by resting state fMRI. *Neuroimage* **59**, 3548–3562 (2012).
33. Y. Benjamini, Y. Hochberg, Controlling the false discovery rate: A practical and powerful approach to multiple testing. *J. R. Stat. Soc. B* **57**, 289–300 (1995).
34. J. J. Maller *et al.*, Revealing the hippocampal connectome through super-resolution 1150-direction diffusion MRI. *Sci. Rep.* **9**, 2418 (2019).
35. F. Latini *et al.*, Segmentation of the inferior longitudinal fasciculus in the human brain: A white matter dissection and diffusion tensor tractography study. *Brain Res.* **1675**, 102–115 (2017).
36. N. Kanwisher, G. Yovel, The fusiform face area: A cortical region specialized for the perception of faces. *Philos. Trans. R. Soc. Lond. B Biol. Sci.* **361**, 2109–2128 (2006).
37. B. Rossion, C. Schiltz, M. Crommelinck, The functionally defined right occipital and fusiform "face areas" discriminate novel from visually familiar faces. *Neuroimage* **19**, 877–883 (2003).
38. R. J. Harris, G. E. Rice, A. W. Young, T. J. Andrews, Distinct but overlapping patterns of response to words and faces in the fusiform gyrus. *Cereb. Cortex* **26**, 3161–3168 (2016).
39. E. Mandonnet, A. Nouet, P. Gatignol, L. Capelle, H. Duffau, Does the left inferior longitudinal fasciculus play a role in language? A brain stimulation study. *Brain* **130**, 623–629 (2007).
40. G. Herbet, I. Zemmoura, H. Duffau, Functional anatomy of the inferior longitudinal fasciculus: From historical reports to current hypotheses. *Front. Neuroanat.* **12**, 77 (2018).
41. C. Semenza, Naming with proper names: The left temporal pole theory. *Behav. Neurol.* **24**, 277–284 (2011).
42. R. J. Von Der Heide, L. M. Skipper, I. R. Olson, Anterior temporal face patches: A meta-analysis and empirical study. *Front. Hum. Neurosci.* **7**, 17 (2013).
43. V. Troiani, C. C. Dougherty, A. M. Michael, I. R. Olson, Characterization of face-selective patches in orbitofrontal cortex. *Front. Hum. Neurosci.* **10**, 279 (2016).
44. E. Barat, S. Wirth, J.-R. Duhamel, Face cells in orbitofrontal cortex represent social categories. *Proc. Natl. Acad. Sci.* **115**, E11158–E11167 (2018).
45. T. Tsukiura, R. Cabeza, Remembering beauty: Roles of orbitofrontal and hippocampal regions in successful memory encoding of attractive faces. *Neuroimage* **54**, 653–660 (2011).
46. K. A. Khan, S. K. Jain, V. D. Sinha, J. Sinha, Preoperative diffusion tensor imaging: A landmark modality for predicting the outcome and characterization of supratentorial intra-axial brain tumors. *World Neurosurg.* **124**, e540–e551 (2019).
47. N. Viñas-Guasch, Y. J. Wu, The role of the putamen in language: A meta-analytic connectivity modeling study. *Brain Struct. Funct.* **222**, 3991–4004 (2017).
48. F. Latini, New insights in the limbic modulation of visual inputs: The role of the inferior longitudinal fasciculus and the Li-Am bundle. *Neurosurg. Rev.* **38**, 179–189, discussion 189–190 (2015).
49. O. Baumann, J. B. Mattingley, Functional organization of the parahippocampal cortex: Dissociable roles for context representations and the perception of visual scenes. *J. Neurosci.* **36**, 2536–2542 (2016).
50. C. B. Kirwan, C. E. Stark, Medial temporal lobe activation during encoding and retrieval of novel face-name pairs. *Hippocampus* **14**, 919–930 (2004).
51. K. Duncan, A. Tompary, L. Davachi, Associative encoding and retrieval are predicted by functional connectivity in distinct hippocampal area CA1 pathways. *J. Neurosci.* **34**, 11188–11198 (2014).
52. M. L. Schlichting, D. Zeithamova, A. R. Preston, CA1 subfield contributions to memory integration and inference. *Hippocampus* **24**, 1248–1260 (2014).

53. J. Chen, R. K. Olsen, A. R. Preston, G. H. Glover, A. D. Wagner, Associative retrieval processes in the human medial temporal lobe: Hippocampal retrieval success and CA1 mismatch detection. *Learn. Mem.* **18**, 523–528 (2011).
54. K. Duncan, N. Ketz, S. J. Inati, L. Davachi, Evidence for area CA1 as a match/mismatch detector: A high-resolution fMRI study of the human hippocampus. *Hippocampus* **22**, 389–398 (2012).
55. G. A. Kerchner *et al.*, Hippocampal CA1 apical neuropil atrophy and memory performance in Alzheimer's disease. *Neuroimage* **63**, 194–202 (2012).
56. T. Bartsch *et al.*, Focal lesions of human hippocampal CA1 neurons in transient global amnesia impair place memory. *Science* **328**, 1412–1415 (2010).
57. C. La *et al.*, Hippocampal CA1 subfield predicts episodic memory impairment in Parkinson's disease. *Neuroimage Clin.* **23**, 101824 (2019).
58. M. M. Zeineh, S. A. Engel, P. M. Thompson, S. Y. Bookheimer, Unfolding the human hippocampus with high resolution structural and functional MRI. *Anat. Rec.* **265**, 111–120 (2001).
59. A. J. Bastos-Leite *et al.*, Hippocampal sulcus width and cavities: Comparison between patients with Alzheimer disease and nondemented elderly subjects. *AJNR Am. J. Neuroradiol.* **27**, 2141–2145 (2006).
60. N. L. Rempel-Clower, S. M. Zola, L. R. Squire, D. G. Amaral, Three cases of enduring memory impairment after bilateral damage limited to the hippocampal formation. *J. Neurosci.* **16**, 5233–5255 (1996).
61. Y.-Z. Huang, J. C. Rothwell, R.-S. Chen, C.-S. Lu, W.-L. Chuang, The theoretical model of theta burst form of repetitive transcranial magnetic stimulation. *Clin. Neurophysiol.* **122**, 1011–1018 (2011).
62. Y.-Z. Huang, M. J. Edwards, E. Rounis, K. P. Bhatia, J. C. Rothwell, Theta burst stimulation of the human motor cortex. *Neuron* **45**, 201–206 (2005).
63. M. Kirkovski *et al.*, A systematic review of the neurobiological effects of theta-burst stimulation (TBS) as measured using functional magnetic resonance imaging (fMRI) OSF Preprints (2020). 10.31219/osf.io/tbpx2 (Accessed 1 October 2020).
64. D. T. Corp *et al.*; 'Big TMS Data Collaboration', Large-scale analysis of interindividual variability in theta-burst stimulation data: Results from the 'Big TMS Data Collaboration'. *Brain Stimul.* **13**, 1476–1488 (2020).
65. S. Rossi, M. Hallett, P. M. Rossini, A. Pascual-Leone; Safety of TMS Consensus Group, Safety, ethical considerations, and application guidelines for the use of transcranial magnetic stimulation in clinical practice and research. *Clin. Neurophysiol.* **120**, 2008–2039 (2009).
66. A. J. Lerner, E. M. Wassermann, D. I. Tamir, Seizures from transcranial magnetic stimulation 2012-2016: Results of a survey of active laboratories and clinics. *Clin. Neurophysiol.* **130**, 1409–1416 (2019).
67. Y. H. Chou, V. Ton That, A. Y. Chen, M. Sundman, Y.-Z. Huang, TMS-induced seizure cases stratified by population, stimulation protocol, and stimulation site: A systematic literature search. *Clin. Neurophysiol.* **131**, 1019–1020 (2020).
68. S. Rossi *et al.*, Safety and recommendations for TMS use in healthy subjects and patient populations, with updates on training, ethical and regulatory issues: Expert guidelines. *Clin. Neurophysiol.* **132**, 269–306 (2020).
69. S. Weintraub *et al.*, Version 3 of the Alzheimer disease centers' neuropsychological test battery in the uniform data set (UDS). *Alzheimer Dis. Assoc. Disord.* **32**, 10–17 (2018).
70. R. J. Ivnik *et al.*, The Auditory-Verbal Learning Test (AVLT): Norms for ages 55 years and older. *Psychol. Assess.* **2**, 304–312 (1990).
71. A. J. Jak *et al.*, Quantification of five neuropsychological approaches to defining mild cognitive impairment. *Am. J. Geriatr. Psychiatry* **17**, 368–375 (2009).
72. R. C. Petersen, J. C. Morris, Mild cognitive impairment as a clinical entity and treatment target. *Arch. Neurol.* **62**, 1160–1163, discussion 1167 (2005).
73. J. Larson, E. Munkácsy, L. T. P. Theta-burst, Theta-burst LTP. *Brain Res.* **1621**, 38–50 (2015).
74. J. J. Borckardt, Z. Nahas, J. Koola, M. S. George, Estimating resting motor thresholds in transcranial magnetic stimulation research and practice: A computer simulation evaluation of best methods. *J. ECT* **22**, 169–175 (2006).
75. P. Fried *et al.*, Relationship of active to resting motor threshold influences the aftereffects of theta-burst stimulation *Brain Stimul.* **12**, 465 (2019).
76. F. Duecker, A. T. Sack, Rethinking the role of sham TMS. *Front. Psychol.* **6**, 210 (2015).
77. J. Veraart, E. Fieremans, I. O. Jelescu, F. Knoll, D. S. Novikov, Gibbs ringing in diffusion MRI. *Magn. Reson. Med.* **76**, 301–314 (2016).
78. J. L. Andersson, S. Skare, J. Ashburner, How to correct susceptibility distortions in spin-echo echo-planar images: Application to diffusion tensor imaging. *Neuroimage* **20**, 870–888 (2003).
79. J. L. R. Andersson, S. N. Sotiropoulos, An integrated approach to correction for off-resonance effects and subject movement in diffusion MR imaging. *Neuroimage* **125**, 1063–1078 (2016).
80. J. V. Manjón *et al.*, Diffusion weighted image denoising using overcomplete local PCA. *PLoS One* **8**, e73021 (2013).
81. N. J. Tustison *et al.*, N4ITK: Improved N3 bias correction. *IEEE Trans. Med. Imaging* **29**, 1310–1320 (2010).
82. J. E. Iglesias *et al.*; Alzheimer's Disease Neuroimaging Initiative, A computational atlas of the hippocampal formation using ex vivo, ultra-high resolution MRI: Application to adaptive segmentation of in vivo MRI. *Neuroimage* **115**, 117–137 (2015).
83. M. Moscovitch, R. Cabeza, G. Winocur, L. Nadel, Episodic memory and beyond: The Hippocampus and neocortex in transformation. *Annu. Rev. Psychol.* **67**, 105–134 (2016).
84. B. Jeurissen, J.-D. Tournier, T. Dhollander, A. Connelly, J. Sijbers, Multi-tissue constrained spherical deconvolution for improved analysis of multi-shell diffusion MRI data. *Neuroimage* **103**, 411–426 (2014).
85. A. Nummenmaa *et al.*, Targeting of white matter tracts with transcranial magnetic stimulation. *Brain Stimul.* **7**, 80–84 (2014).
86. A. Thielscher, A. Antunes, G. B. Saturnino, Field modeling for transcranial magnetic stimulation: A useful tool to understand the physiological effects of TMS? *Annu. Int. Conf. IEEE Eng. Med. Biol. Soc.* **2015**, 222–225 (2015).
87. K. Worsley, "Statistical analysis of activation images" in *Functional MRI: An introduction to methods*, P. Jezzard, P. M. Matthews, S. M. Smith, Eds. (Oxford Scholarship Online, 2000).
88. B. B. Biswal *et al.*, Toward discovery science of human brain function. *Proc. Natl. Acad. Sci. U.S.A.* **107**, 4734–4739 (2010).
89. S. H. Tak, S. H. Hong, Face-name memory in Alzheimer's disease. *Geriatr. Nurs.* **35**, 290–294 (2014).
90. M. Minear, D. C. Park, A lifespan database of adult facial stimuli. *Behav. Res. Methods Instrum. Comput.* **36**, 630–633 (2004).
91. S. Whitfield-Gabrieli, A. Nieto-Castanon, Conn: A functional connectivity toolbox for correlated and anticorrelated brain networks. *Brain Connect.* **2**, 125–141 (2012).